

Electrodeposition of Fe-Zn, Fe-Mn and Fe-Zn-Mn alloys on steel from ionic liquids

C. Akdogan^a, O. F. Bakkaloglu^a, M. Bedir^a, P. Y. Erdogan^b, A. Yavuz^{*c}

^a*Department of Engineering Physics, Faculty of Engineering, Gaziantep University, Sehitkamil, Gaziantep, 27310, Turkey*

^b*Department of Chemistry, Faculty of Science and Literature, Gaziantep University, Sehitkamil, Gaziantep, 27310, Turkey*

^c*Department of Metallurgical and Materials Engineering, Faculty of Engineering, Gaziantep University, Sehitkamil, Gaziantep, 27310, Turkey*

Ionic liquids containing solely anions and cations (without solvent) have been employed as metals and alloys electrodeposition baths. Growth conditions have a considerable impact on the surface properties of coatings. In this study, electrodes composed of Fe alloys such as Fe-Zn, Fe-Mn, and Fe-Zn-Mn were produced on the surface of steel using an ionic liquid solution. Thin film coatings with nanostructures were obtained uniformly on the steel surface. A scanning electron microscope, an energy dispersive spectrometer, X-Ray Diffraction and a Fourier Transform Infrared Spectrometer were used to characterize the surface morphologies, compositions, and structures of the synthesized coatings. The corrosion behavior of the alloy coatings was determined by linear sweep voltammetry.

(Received January 20, 2022; Accepted May 6, 2022)

Keywords: Electrodeposition, Fe alloys, Steel, Ionic liquids, Deep eutectic solvents

1. Introduction

Corrosion is typically defined as the degradation of metals as a result of an electrochemical reaction [1]. Corrosion is an oxidation reaction that happens mostly on the surface of metal-based materials. However, oxidation of metals or alloys may act as a barrier to further oxidation [2]. A passive layer is formed when oxidation of materials results in a layer that prevents further oxidation of the bulk material. When corrosion occurs on the surface of bronze and aluminium, it appears as a thin greenish layer known as patina and alumina, respectively [3][4]. In stainless steel, the creation of a Cr₂O₃ layer can be detected, and this layer is also a passive layer. Zinc has a passive layer, and the coating of metals/alloys with zinc, referred to as galvanisation [5], is a regular occurrence in daily life. Corrosion on the surface of these four very recognizable metals eliminates interaction with the external environment and protects the lower surfaces. However, rust in iron, which is the most common engineering metal, exfoliates from the surface of the metal [6]. Keeping this layer on the surface of the iron (or steel) can help prevent additional rusting. This spongy structure, however, was unable to prevent the metal from coming into contact with the air or the surrounding environment [7]. Due to the fact that rust is poured from the iron surface, the remaining lower portions of the iron metal chemically react with the environment and oxidize anew; this process continues until the iron metal is fully consumed [8]. Corrosion with wear exist indeed as the main important factor of energy and material losses in mechanical and chemical processes [9]. Iron is the most widely utilized metal, accounting for more than half of all metals produced globally [10]. Today, the widespread usage of iron-based metals, particularly in the automotive, ship, and aircraft industries, has spawned research into corrosion prevention [11].

The most straightforward method is to protect metal objects from moisture, so delaying corrosion. However, after a period of time, when this procedure is no longer sufficient, methods such as painting are applied. While these procedures appear to be effective in the short term, they may soon be overtaken by electrodeposition methods that delay metal corrosion [12]. When

* Corresponding author: ayavuz@gantep.edu.tr
<https://doi.org/10.15251/DJNB.2022.172.589>

corrosion of metals is postponed; the labour, time, and economic losses associated with corrosion could be minimized [13]. Corrosion occurs when the microstructure of metals/alloys reacts with oxygen and water. As a result of the absence of water-containing moisture, areas with arid climates are less prone to corrosion. Because of the oxygen in humid environments, metals are more susceptible to rust [14]. In light of current economic conditions, it has been determined that the losses caused by rust exceed the expense of working on corrosion-prevention technologies. In corrosion-resistance investigations, electrodeposition of a single element or alloys of two or more elements was utilized on the surfaces of materials subjected to adverse environmental conditions such as moisture or chemical particles. To investigate corrosion change, iron alloys (Fe-Zn, Fe-Mn, and Fe-Zn-Mn) were electrochemically coated on steel, in this study.

Numerous research on the electrodeposition of iron and iron alloys in aqueous solution have been conducted, according to literature searches [15]. To mitigate the detrimental effects of aqueous solutions (for example, hydrogen evolution during cathodic electrodeposition), the thin films using ionic liquid were grown [16]. The ionic liquid used in this study was created by mixing choline chloride and ethylene glycol in a 1:2 ratio called Ethaline. Prior to coating a steel from this ionic liquid electrolyte, any aqueous residues in the ionic liquid were eliminated by heating to around 60 °C. Additionally, the reference, counter, and working electrodes were dried with hot air to remove any remaining moisture on their surfaces. Electrodeposition of alloys (Fe-Zn, Fe-Mn, and Fe-Zn-Mn) was accomplished by applying a constant potential to an ionic liquid containing salts of Fe-Zn, Fe-Mn and Fe-Zn-Mn, respectively. The electrochemical, morphological, structural, and compositional properties of thin films (iron-based alloys) grown on steel were determined using a cyclic voltammogram, a scanning electron microscope, an energy dispersive spectrometer, an X-Ray Diffraction, and a Fourier Transform Infrared Spectrometer.

2. Experimental

2.1. Materials

Without further purification, NaCl (Merck, 90%), FeSO₄·7H₂O (Merck, 99.5%), MnCl₂·4H₂O (Merck, 99%), ZnCl₂ (Merck, 98%), ethylene glycol (C₂H₆O₂, Merck, 99%) (EG) and choline chloride (HOC₂H₄N(CH₃)₃Cl, Merck, 98%) (ChCl) were utilized. Ethaline ionic liquid was prepared by mixing ethylene glycol (liquid) and choline chloride in a molar ratio of 1:2. To make Ethaline ionic liquid, the molar ratio of ethylene glycol (liquid) to choline chloride was 1:2. Heating the mixture to 55 °C produced a homogenous liquid solution in about 30 minutes.

2.2. Preparation of coating electrodes

To make a deposition electrolyte, Ethaline ionic liquids containing individually FeSO₄-ZnCl₂, FeSO₄-MnCl₂, and a mixture of FeSO₄, ZnCl₂, and MnCl₂ were utilized. The steel substrate was cleaned with deionized water and dried after being ground with sandpapers (200, 800, 1500 mesh). Steel substrates were immersed in an Ethaline solution including FeSO₄ and ZnCl₂ for Fe-Zn coating, FeSO₄ and MnCl₂ for Fe-Mn coating, and FeSO₄, ZnCl₂, and MnCl₂ for Fe-Zn-Mn coating. Electrodeposition was performed by applying -1.6 V for 300 seconds at a temperature of 55 °C. All of the coatings were grown separately on the steel surface in this manner. When the working electrode was ground steel, a platinum reference electrode and a platinum coated titanium counter electrode were utilized. Due to the absence of water in ionic liquid, an Ag-AgCl reference electrode containing aqueous solution was not used during the electrodeposition of the films.

2.3. Characterization of the electrodes

The chemical structures of uncoated steel were determined using FT-IR (Perkin Elmer, Connecticut, USA), and the results were compared to the chemical structures of Fe-Zn, Fe-Mn, and Fe-Zn-Mn coated steel substrates. SEM morphological investigations of bare steel, Fe-Zn, Fe-Mn, and Fe-Zn-Mn alloy thin films on steel were performed (ZEISS Gemini FEGSEM 300, Germany). X-ray diffraction was used to determine the phase of the prepared thin films (XRD). The electrodes in this work were electrochemically characterized using a potentiostat equipped with a three-electrode setup. The VersaSTAT3 (Oak Ridge, USA) potentiostat consisted of a

reference, a working, and a counter electrode. In this study, coated steels were subjected to potentiodynamic polarization with 3.5 weight % NaCl to understand the corrosion process of the electrodes produced. In aqueous solution, an Ag-AgCl reference electrode was employed to maintain a consistent potential throughout the experiment. Steel (coated or uncoated) working and platinum coated titanium counter electrodes were utilized. The rationale for not using the Ag-AgCl (3 M KCl) reference electrode in the ionic liquid medium is because the water in the Ag-AgCl reference electrode can mix with the ionic liquid, altering the measurement potential. When the electrodes were cycled in aqueous NaCl solution, Ag/AgCl (with saturated KCl solution) was employed as a reference electrode.

3. Results and discussion

3.1. Growth of Fe-Zn, Fe-Mn and Fe-Zn-Mn alloy films

Using a cyclic voltammogram, the steel working electrode was immersed in Ethaline ionic liquid to investigate the growth conditions of Fe-Zn, Fe-Mn, and Fe-Zn-Mn on steel. The cyclic voltammogram curves of a bare steel electrode in pure Ethaline solution (red line of Figure 1a) and in Ethaline solution containing both Fe^{2+} and Zn^{2+} salts (black line of Figure 1b) and Fe^{2+} and Mn^{2+} salts are shown (red line of Figure 1b). All electrolytes' cyclic voltammograms were started at 0 V and scanned to -1.7 V, and then scanned back to 0.5 V at the same scan rate. When a bare steel electrode was immersed in Ethaline ionic liquid at 0 V, it oxidized because the ionic liquid can directly oxidize the steel. The direction of scanning was from 0 V to the negative side. Steel oxidation was halted at around -0.5 V. Between -0.5 V and around -1.3 V, no redox reaction occurred since the current through steel was around 0 A (red line in Figure 1a), indicating that there were no ions that could be reduced in Ethaline at this potential range. Normally, Ethaline did not contain any metal salt at the start (before polarisation). As the steel working electrode did not oxidize again when the cycle potential was increased from -1.7 V to roughly -0.4 V, current was around 0 V and no reduction or oxidation occurred. As no oxidation peak was recorded following the reduction at roughly -1.7 V, it may be concluded that the reduction happened as a result of hydrogen evolution. At approximately -0.45 V, steel was oxidized (in red line of Figure 1a).

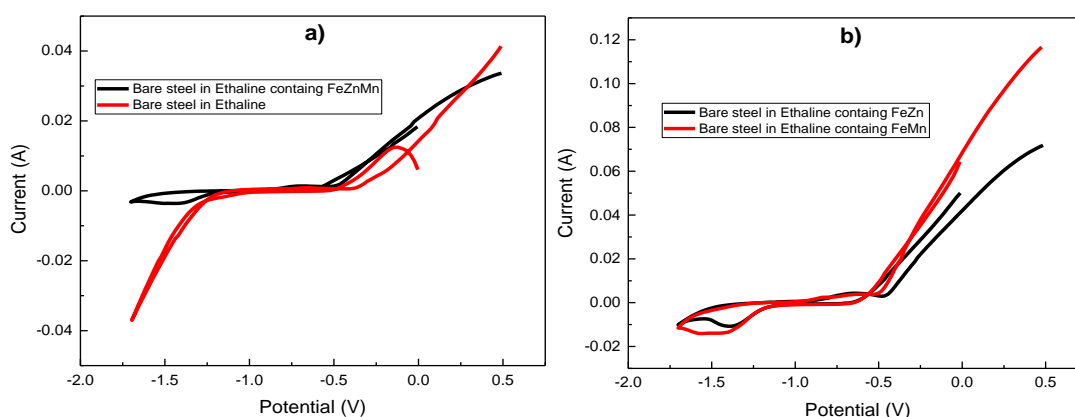


Fig. 1. (a) Cyclic voltammogram curve of bare steel working electrode in pure Ethaline solution (black line) and in Ethaline solution containing Fe^{2+} , Zn^{2+} and Mn^{2+} ions (red line); (b) Cyclic voltammogram curve of bare steel working electrode in Ethaline solutions containing Fe^{2+} and Zn^{2+} (black line) and Fe^{2+} and Mn^{2+} (red line). $v = 20 \text{ mV s}^{-1}$.

When bare steel was immersed in Ethaline containing Fe and Mn salts (red line in Figure 1b), the steel electrode reduced at potentials ranging from 0 to -0.5 V. This is due to the reduction of the steel electrode observed when bare steel was cycled in pure Ethaline. There was no appreciable current between -0.5 V and roughly -1.2 V, indicating that there was no reduction or oxidation of the steel in Ethaline containing Fe and Mn salts. Then, a slight reduction peak

occurred between -1.2 V and roughly -1.4 V, and there is no current changing between -1.4 V and -1.6 V. This cathodic current (reduction) happened as a result of Mn^{2+} and/or Fe^{2+} ion reduction. Between -1.4 V to approximately -0.8 V, current was near zero, with no evidence of reduction or oxidation. At around -0.7 V, a tiny oxidation peak was noticed, which could be due to film dissolution. Finally, an oxidation was observed between -0.5 V and 0.5 V. This peak cannot provide information on film dissolution since steel can oxidize in this range of potentials.

When bare steel is examined in Ethaline containing both Fe^{2+} and Zn^{2+} -based salts (black line in Figure 1b), an oxidation in bare steel is found between 0 and -0.5 V. The cyclic voltammogram pattern for steel in Ethaline containing iron and zinc salt (black line in Figure 1b) is similar to the pattern for steel in Ethaline containing Fe^{2+} and Mn^{2+} salt (red line of Figure 1b). As a result, both electrolytes undergo identical reduction and oxidation. When bare steel was immersed in Ethaline containing Fe^{2+} , Zn^{2+} , and Mn^{2+} salts (black line in Figure 1a), the current of steel electrode decreased between 0 and approximately -0.5 V. Due to the fact that the ampere is zero when scanning between -0.5 V and approximately -1.25 V, there was no reduction or oxidation of the salt or steel electrode at these voltages. Between -1.25 and -1.7 V, a decrease in voltage was noticed, which could be due to the deposition of the alloy-based coating. Thus, by applying -1.6 V, these films (Fe-Zn, Fe-Mn, and Fe-Zn-Mn) may be formed.

3.2. Characterisation of the electrodes

Fe-Zn, Fe-Mn, and Fe-Zn-Mn films were electrodeposited on steel surfaces using Ethaline containing their salts. Before disclosing their corrosion behavior, these electrodes were characterized. EDAX and SEM analyses were used to establish the coatings' elemental and morphological compositions [17]. SEM pictures of Fe-Zn, Fe-Mn, and Fe-Zn-Mn alloys coated steel electrodeposited from an ionic liquid media are shown in Figure 2. SEM picture of steel inset in Figure 2a reveals scratches on the steel surface caused by the grinding operation. Clustered nanoparticles were found in Figure 2b's SEM image of a Fe-Zn coating on steel. The SEM picture of Fe-Mn in Figure 2c resembles a cloudy sky. On the other hand, as illustrated in Figure 2d, the SEM picture of Fe-Zn-Mn electrodeposited on steel resembles an uneven heterogeneous sheet.

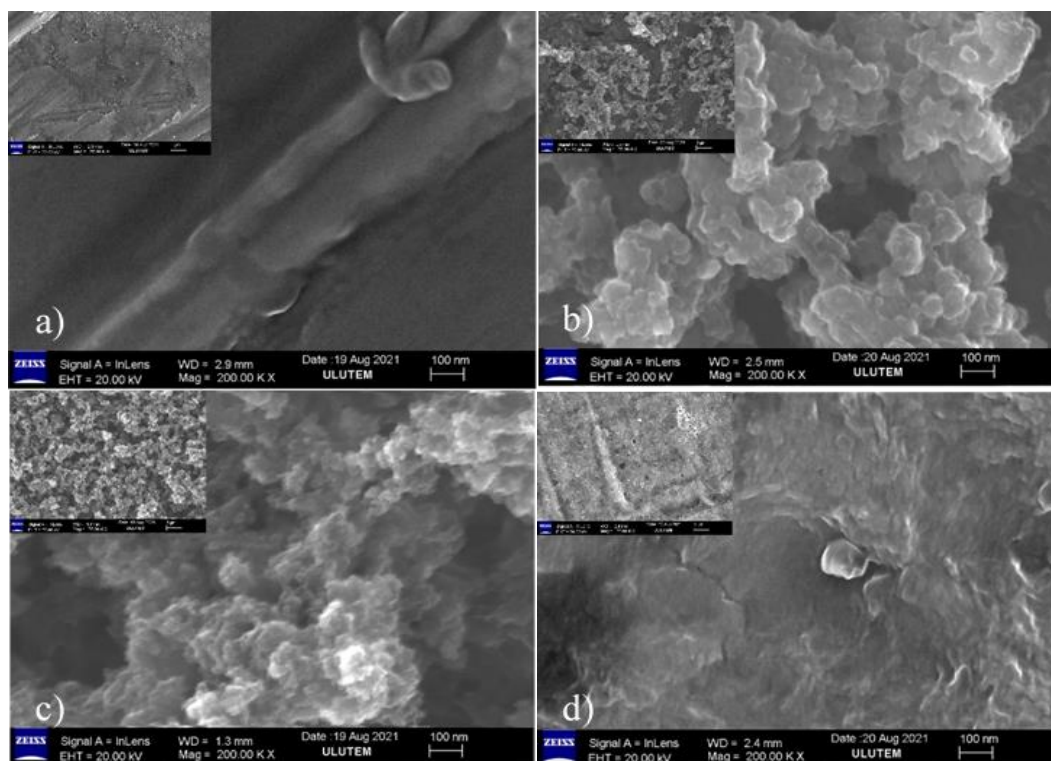


Fig. 2. SEM image of a) bare steel, b) electrodeposited Fe-Zn based alloy on steel; c) electrodeposited Fe-Mn based alloy on steel and; d) electrodeposited Fe-Zn-Mn based alloy on steel. The films were obtained potentiostatically from Ethaline ionic liquid.

Before presenting the XRD, FTIR, and corrosion data for the coating, the EDAX analysis of uncoated and alloy coated electrodes are presented in Table 1. On steel, Fe-Zn and Fe-Mn coatings contain 3.5 % Zn and 3.5 % Mn, respectively. Both of them have an Fe content of 96.5 %, as steel is mostly composed of iron. Due to the thinness of the coatings, EDAX was able to detect significantly the underlying iron. The elemental composition of the Fe-Zn-Mn alloy indicates that it contains 1.7 % Mn and 0.5 % Zn.

Table 1: Elemental ratio in Fe-Zn, Fe-Mn and Fe-Zn-Mn alloys electrodeposited on steel.

Alloys →	Fe-Zn	Fe-Mn	Fe-Zn-Mn
Element ↓	Wt%	Wt%	Wt%
Mn	0	3.5	1.7
Fe	96.5	96.5	97.8
Zn	3.5	0	0.5

XRD is a technique for determining the crystal structure of a material using the scattered X-rays in various directions [18]. XRD was used to analyze the crystal structure of electrochemically deposited coatings on steel. Figure 3 shows the XRD patterns of the bare steel electrode with Fe-Zn, Fe-Mn, and Fe-Zn-Mn alloy samples put on it. Because the films are thin and the XRD results are dominated by the steel substrate, the XRD peaks of Fe-Zn, Fe-Mn, and Fe-Zn-Mn alloys coated steel were similar to those of bare steel electrode (Figure 3). The peaks of the supplied electrodes correspond to the steel orientations (110), (200), and (211) [19].

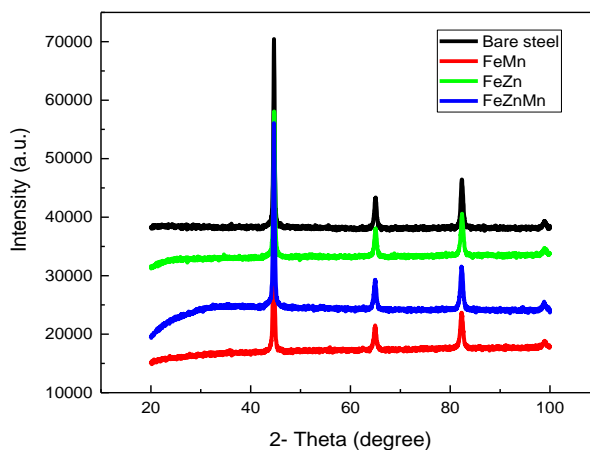


Fig. 3. X-ray diffraction (XRD) patterns of a) bare steel; b) Fe-Mn; c) Fe-Zn and; d) Fe-Zn-Mn coated steel.

FTIR is a technique for obtaining the infrared absorption and emission spectra of a substance [20]. Figure 4 illustrates the vibration spectra of modified and untreated steel electrodes. Figure 4a illustrates the FTIR spectrum of uncoated steel. In the spectra of bare steel, there is only one peak about 410 cm^{-1} (black line of Figure 4a). The FTIR spectrum of the Fe-Mn alloy electrochemically coated onto the steel is shown in Figure 4b (red line). The Fe-Mn alloy's FTIR spectra (Figure 4b) showed peaks at $451, 700, 1111, 1586,$ and 3255 cm^{-1} . Figure 4c depicts the FTIR spectrum of the Fe-Zn alloy. When the Fe-Zn alloy's FTIR spectrum is investigated, it is discovered to have peaks around $450, 500, 700, 1080$ and 1580 cm^{-1} (green line, Figure 4c). These peaks indicate that the electrochemically formed alloy coatings may be in the form of their oxide

or hydroxide in nature. Figure 4d depicts the FTIR spectrum of the Fe-Zn-Mn ternary alloy. Its peaks are located at around 665, 1634, 1653, and 1700, 2313, and 3407 cm^{-1} (blue line, Figure 4d).

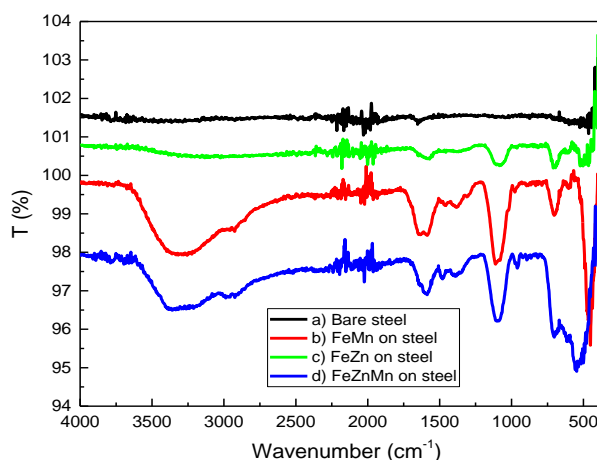


Fig. 4. FTIR spectra of a) bare steel electrode (black line); b) Fe-Mn (red line); c) Fe-Zn (green line); and d) Fe-Zn-Mn (blue line) alloy deposited on steel electrode.

3.3. Corrosion study of the electrodes

E_{corr} and I_{corr} values can be computed from the Tafel values by intersecting the oxidation and reduction lines of the corrosion current density and corrosion potential on the Tafel plot. Tafel plots were obtained by immersing Fe-Zn, Fe-Mn, and Fe-Zn-Mn alloys coated on steel (Figure 5a) and platinum (Figure 5b) substrates in an aqueous 3.5 wt.% NaCl solution. To examine the corrosion behavior of Fe-Zn, Fe-Mn, and Fe-Zn-Mn coated steel and platinum electrodes generated electrochemically, they were compared with the corrosion behaviour of uncoated steel and platinum electrodes. The Tafel plot of Fe-Zn, Fe-Mn, and Fe-Zn-Mn alloys coated on steel is shown in Figure 5a. Corrosion current and potential values of modified electrodes in 3.5 wt% NaCl media can be estimated using the logarithm of current in linear sweep voltammeter responses. Figure 5b shows Tafel plots of the bare platinum electrode and electrochemically deposited Fe-Zn, Fe-Mn, and Fe-Zn-Mn alloys on the platinum substrate in a 3.5 percent NaCl solution (25 °C).

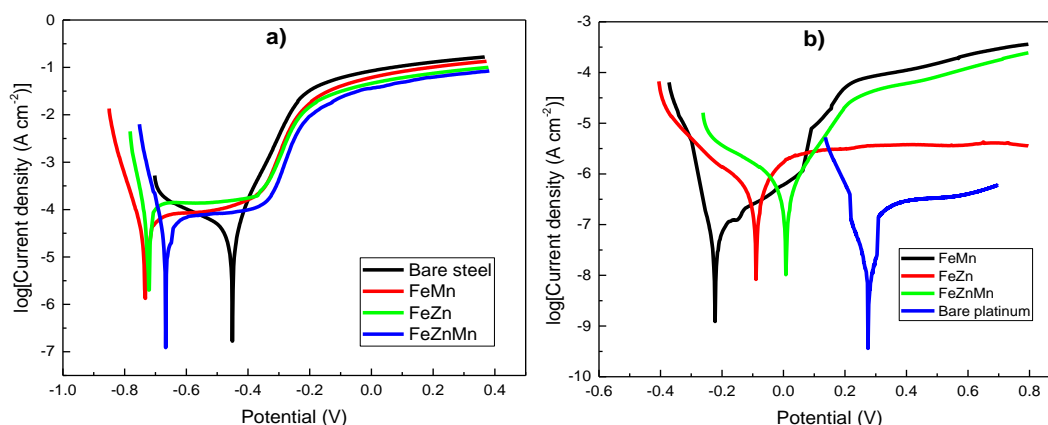


Fig. 5. a) Potentiodynamic polarization responses of bare steel (black line) electrode, iron manganese alloy (red line), iron zinc alloy (green line), and iron, zinc and manganese alloy (blue line) electrodes electrochemically coated on steel substrate in 3.5% NaCl solution at 25 °C. b) Potentiodynamic polarization responses behaviour of bare platinum (blue line) electrode, iron manganese alloy (black line), iron zinc alloy (red line), and iron, zinc and manganese alloy (green line) alloy electrodes electrochemically coated on platinum substrate in 3.5% NaCl solution at 25 °C.

I_{corr} is a critical metric for determining the kinetics of corrosion reactions. The lower the I_{corr} value, the slower the corrosion rate and the greater the material's corrosion resistance [21]. Table 2 summarizes the corrosion current and potential of the electrodes utilized in this study. When I_{corr} values of electroplated samples are examined, it is discovered that the corrosion rate of bare steel did not rise after it was coated with alloys, owing to the fact that the corrosion responses obtained using linear sweep voltammetry were dominated by the steel substrate. As a result, the alloys were electrodeposited on the Pt surface to demonstrate the coating effect. All alloy coatings had a lower corrosion current (less than 1 A cm^{-2}) than steel (63 A cm^{-2}). Fe-Zn, Fe-Mn, and Fe-Zn-Mn alloys coated on steel can be used to protect steel against corrosion.

Table 2. Electrochemical parameters of Fe-Zn, Fe-Mn, and Fe-Zn-Mn alloys synthesized electrochemically on steel and platinum electrode and transferred into 3.5% NaCl solution. The data given in Figure 5a were used for I_{corr} and E_{corr} of the electrodes.

Electrode	$I_{\text{corr}}/\mu\text{A cm}^{-2}$	E_{corr} vs. Ag-AgCl/V
Bare steel	63	-0.487
Fe-Zn on steel	56	-0.722
Fe-Mn on steel	104	-0.786
Fe-Zn-Mn on steel	75	-0.665
Fe-Zn on platinum	0.62	-0.081
Fe-Mn on platinum	0.11	-0.224
Fe-Zn-Mn on platinum	0.76	+0.023

4. Conclusions

The structure and corrosion behavior of electrodeposited Fe-Zn, Fe-Mn, and Fe-Zn-Mn alloys on steel electrodes were examined in this study. Between -1.7 V and +0.5 V, the deposition conditions of alloys on steel from an ionic liquid media were determined using a cyclic voltammogram. The alloys were produced potentiostatically by applying -1.6 V for 300 seconds. The structure of the thin films generated in this manner was next investigated. Tafel curves, X-ray, FTIR, SEM and EDAX were used to determine the properties of the samples. Corrosion tests on electrodeposited Fe-Zn, Fe-Mn, and Fe-Zn-Mn alloys on steel surfaces were conducted in 3.5 wt.% NaCl. The I_{corr} values indicated that alloy coatings had no effect on the corrosion resistance of steel. When platinum was coated, it was discovered that the I_{corr} value of alloys decreased. As a result, electrodeposition of Fe-Zn, Fe-Mn, and Fe-Zn-Mn alloys can provide corrosion protection for steel.

Acknowledgments

The authors wish to express their gratitude to the Gaziantep University Scientific Research Unit (MF.YLT.18.16).

References

- [1] A. P. I. Popoola, O. E. Olorunniwo, O. O. Ige, " Dev. Corros. Prot., vol. 13, no. 4, pp. 241-270, 2014; <https://doi.org/10.5772/57420>
- [2] H. Tamura, Corros. Sci., vol. 50, no. 7, pp. 1872-1883, 2008; <https://doi.org/10.1016/j.corsci.2008.03.008>
- [3] I. O. Wallinder, X. Zhang, S. Goidanich, N. Le Bozec, G. Herting, and C. Leygraf, Sci. Total Environ., vol. 472, pp. 681-694, 2014; <https://doi.org/10.1016/j.scitotenv.2013.11.080>
- [4] T. Li, X. G. Li, C. F. Dong, and Y. F. Cheng, J. Mater. Eng. Perform., vol. 19, no. 4, pp. 591-598, 2010; <https://doi.org/10.1007/s11665-009-9506-7>
- [5] L. Cao, Y. Wan, Y. Li, and S. Yang, Lubr. Sci., vol. 33, no. 6, pp. 325-334, 2021; <https://doi.org/10.1002/ls.1555>
- [6] L. S. Selwyn, P. I. Sirois, and V. Argyropoulos, Stud. Conserv., vol. 44, no. 4, pp. 217-232, 1999; <https://doi.org/10.1179/sic.1999.44.4.217>
- [7] S. A. Bradford and J. E. Bringas, Corrosion control, vol. 115. Springer, 1993; <https://doi.org/10.1007/978-1-4684-8845-6>
- [8] F. H. Haynie, ASTM Spec. Tech. Publ., vol. STP, no. 965, pp. 282-289, 1988; <https://doi.org/10.1520/STP25855S>
- [9] R. Suraj, Mater. Today Proc., vol. 42, pp. 842-850, 2020; <https://doi.org/10.1016/j.matpr.2020.11.592>
- [10] "Chemical properties of iron - Health effects of iron - Environmental effects of iron," Lenntech. (Accessed Febr. 17, 2016). Iron [Online], Available <http://www.lenntech.com/periodic/elements/fe.htm>.
- [11] M. Izaki, Mod. Electroplat., vol. 5, 2010; <https://doi.org/10.1002/9780470602638.ch11>
- [12] S. Pandiyarajan, M. Ganesan, A.-H. Liao, S. S. M. Manickaraj, S.-T. Huang, and H.-C. Chuang, Ultrason. Sonochem., vol. 72, p. 105463, 2021; <https://doi.org/10.1016/j.ultsonch.2021.105463>
- [13] H. Wang, J. Xu, X. Du, Z. Du, X. Cheng, and H. Wang, Compos. Part B Eng., vol. 225, p. 109273, 2021; <https://doi.org/10.1016/j.compositesb.2021.109273>
- [14] S. Harsimran, K. Santosh, and K. Rakesh, Proc. Eng., vol. 3, no. 1, pp. 13-24, 2021; <https://doi.org/10.24874/PES03.01.002>
- [15] C. Jiang, M. Feng, M. Chen, K. Chen, S. Geng, and F. Wang, Corros. Sci., vol. 187, p. 109484, 2021; <https://doi.org/10.1016/j.corsci.2021.109484>
- [16] I. El-Hallag, S. Elsharkawy, and S. Hammad, Int. J. Hydrogen Energy, vol. 46, no. 29, pp. 15442-15453, 2021; <https://doi.org/10.1016/j.ijhydene.2021.02.049>
- [17] G. Amo-Duodu et al., Polymers (Basel), vol. 13, no. 24, p. 4323, 2021; <https://doi.org/10.3390/polym13244323>
- [18] Ö. Bedir and T. H. Doğan, Energy Sources, Part A Recover. Util. Environ. Eff., pp. 1-18, 2021; <https://doi.org/10.1080/15567036.2021.1883159>
- [19] D. Aryanto, T. Sudiro, and A. S. Wismogroho, Pist. J. Tech. Eng., vol. 1, no. 2, 2019; <https://doi.org/10.32493/pjte.v1i2.3185>
- [20] R. J. Jadaa, A. N. Abd, and A. A. Khadom, Chem. Pap., pp. 1-12, 2021; <https://doi.org/10.1007/s11696-021-01725-5>
- [21] J. G. and Y. L. Tao Ma, Huirong Li, "Corrosion Behaviour of Cu/Carbon Steel Gradient Material," 2021.